

1 **Studying the effect of solubilizing agents on drug diffusion through the**  
2 **unstirred water layer (UWL) by localized spectroscopy**

3 Massimiliano Pio di Cagno<sup>a,b\*</sup> and Paul C. Stein<sup>c</sup>

4

5 *<sup>a</sup>Department of Pharmacy, Faculty of Mathematics and Natural Sciences, University of Oslo, Norway*

6 *<sup>b</sup>Drug Transport and Delivery Research Group, Department of Pharmacy, University of Tromsø, The*

7 *Arctic University of Norway, Tromsø, Norway*

8 *<sup>c</sup>Department of Physics, Chemistry and Pharmacy, University of Southern Denmark, Odense,*

9 *Denmark*

10

11 \*Corresponding author: Massimiliano Pio di Cagno; Tel: +47 22856598; e-mail:

12 [m.p.d.cagno@farmasi.uio.no](mailto:m.p.d.cagno@farmasi.uio.no)

13

14 **Abstract**

15 An experimental/computational approach has been successfully applied in order to study the  
16 effect of solubilizing vehicles (cyclodextrins and liposomes) on the passive diffusion of four  
17 active pharmaceutical ingredients (API) of different nature (hydrophilic, ionizable and  
18 lipophilic) through an unstirred water layer (UWL) model. This approach allowed the  
19 measurement of flux changes through the UWL and the computational calculation of different  
20 parameters relevant to interpret the interplay within solubilizing vehicles and UWL diffusion.  
21 In the case of cyclodextrin, this approach allowed the determination of free drug diffusivity  
22 ( $D_f$ ), bound drug diffusivity ( $D_b$ ) and the equilibrium constant ( $K$ ). In the case of liposomes,  
23 the experimental approach allowed the determination of the liposomes/water partition  
24 coefficient ( $P_{lip/w}$ ) as well as relative API diffusivity ( $(\overline{D})$ , i.e. the drug diffusion in the  
25 presence of solubilizing agents). This work demonstrates that the presence of solubilizing  
26 vehicles hampers the diffusion of API through UWL due to a combination of reduction in

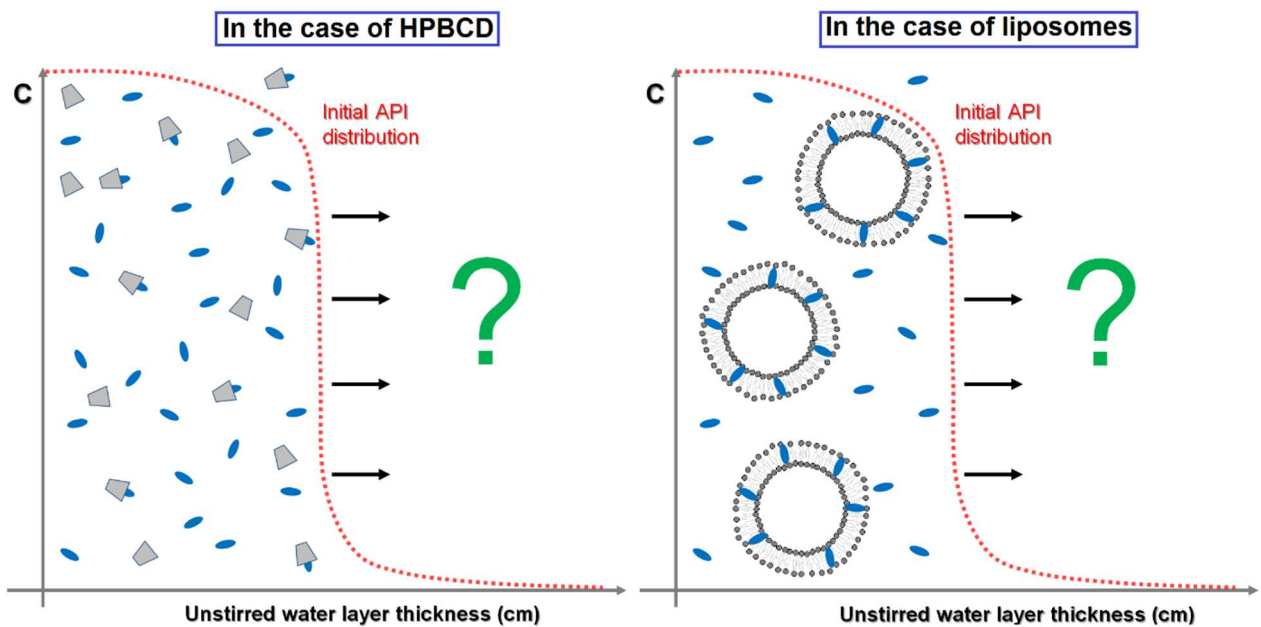
27 relative diffusivity and concentration gradient. These results are highly relevant as they might  
28 help to explain why biological performance of API is affected by the presence of  
29 solubilizing/complexing agents.

30 **Keywords:** Unstirred water layer, passive diffusion, gradient of concentration, solubilizing  
31 agents, cyclodextrin, liposomes.

32

33 **Graphical abstract**

34



35

36

## 37 **1. Introduction**

38 More than 40% of marketed drugs and 90% of new chemical entities under development with  
39 promising pharmaceutical activities suffer from poor water solubility [1]. In an attempt to  
40 increase the biopharmaceutical performance of these compounds one approach that has been  
41 extensively studied in the recent year has been the employment of solubilizing agents [2]  
42 under the assumption that increased apparent aqueous solubility of the drug will result in  
43 increased bioavailability. Since their first descriptions in the middle of last century  
44 cyclodextrins and liposomes have been heavily studied in light of their strong ability to  
45 solubilize lipophilic compounds [3, 4]. Cyclodextrins are capable of solubilizing lipophilic  
46 entities due to inclusion complexes formation [5] whereas liposomes incorporate lipophilic as  
47 well as amphiphilic moieties in the phospholipid bilayers of which liposomes consist of [4].  
48 Even though in most cases these entities are capable of solubilizing poorly soluble substances  
49 of orders of magnitude [6, 7] resulting in a positive enhancement of bioavailability, in some  
50 cases biopharmaceutical performances are reduced [8]. It has been suggested that the  
51 negative influence of some solubilizing agents (dose dependent effect [9]) on  
52 biopharmaceutical performance of drug is related to a reduction in API transport (i.e. mass  
53 transfer) through biological barriers. Furthermore, some studies have emphasized the role of  
54 the unstirred water layer (UWL [10, 11]) as the limiting step of the transport process through  
55 barriers [12, 13]. The UWL represents an additive aqueous layer that covers biological  
56 barriers where conditions of stagnation hold [14] and that drug molecules need to cross before  
57 entering in contact with the lipophilic environment represented by cell membranes [12, 13].  
58 Considering the UWL as a homogeneous environment, where molecules will spontaneously  
59 diffuse through, the flux ( $j$ ) of an API through this layer can be described by Fick's first law  
60 as Eq. 1:

$$j = -D \frac{dc}{dx} \quad \text{Equation 1}$$

61 In this equation, D represents the diffusion coefficient of API molecules in the UWL and  
62  $dc/dx$  the local concentration gradient. Brewster et al. [15] investigated the *effective*  
63 *permeability* of different drugs and hydroxypropyl- $\beta$ -cyclodextrin (HPBCD) through a  
64 parallel artificial membrane permeability assay (PAMPA) in the presence of UWL of  
65 different thickness. They found that, for molecules with high affinity for HPBCD (i.e.  
66 lipophilic) the permeability of the drug was reduced by increased cyclodextrin concentration,  
67 whereas, for compound with low HPBCD-API equilibrium constant (K), no significant  
68 reduction was observed. Dahan et al. [16, 17] tried to describe the interplay between  
69 permeability/complexing agents and UWL with the quasi-equilibrium mathematical model. In  
70 this case they utilized a cellular-based permeability assay (Caco-2), PAMPA and an animal  
71 model in order to investigate the *effective permeability* of drugs in the presence and absence  
72 of cyclodextrins in order to understand the role of UWL in drug permeability in presence of  
73 complexing agents. In accordance with Brewster at al. they have found a correlation between  
74 reduction in drug permeability and HPBCD concentration. Some mechanistic explanations  
75 have been suggested to describe this interesting phenomenon [15-17]. One hypothesis is that  
76 HPBCD reduces the amount of free fraction of drug available, decreasing the concentration  
77 gradient ( $dc/dx$ ) and therefore reducing the net flux of drug molecules through the UWL (Eq.  
78 1) [17]. Another explanation that has been proposed is related to partitioning and  
79 permeability. According to Fine-Shamir et al. [18] the presence of cyclodextrin should reduce  
80 the ability of API molecules to distribute through the lipophilic environment (i.e. reduction in  
81 apparent distribution coefficient) negatively affecting the net transport of the drug through the  
82 whole barrier. Stewart et al. (2017) introduced a new analytical method capable of  
83 discriminating the limiting step in permeability within UWL or the membrane in the presence  
84 of bioavailability-enhancing drug products [19]. They identify two main mechanisms of

85 permeation, in which the API flux through the barrier is influenced by the total concentration  
86 gradient of the drug (i.e. free drug and bound drug) only when the UWL is the limiting step of  
87 the permeation. Even though all these studies indicate UWL as responsible for the reduction  
88 of the overall mass transfer in the presence of solubilizing agents, a proper mechanistic  
89 explanation of the phenomena is still missing. The aim of this work is to experimentally  
90 measure and mathematically describe the diffusion of API molecules through an UWL in the  
91 presence of two types of solubilizing vectors: cyclodextrins and liposomes. In this work we  
92 applied the analytical/computational approach based on temporal resolution of diffusion  
93 profiles in UWL recently introduced by us [20] in order to effectively quantify the changes in  
94 API flux through an UWL in the presence of solubilizing vectors. In this way we could derive  
95 all parameters relevant for the characterization of diffusion process namely, diffusivities,  
96 equilibrium constants and concentration gradients. This new approach is quite unique as it  
97 allows the real-time measurement of relative flux changes, allowing the direct  
98 characterization of all relevant parameters in the UWL. The results obtained in this work  
99 highlight the role that the UWL plays in permeation of drugs, especially when solubilizing  
100 vehicles are present.

## 101 **2. Materials and Methods**

### 102 **2.1 Materials**

103 All buffering agents (sodium dihydrogen phosphate monohydrate ( $\text{NaH}_2\text{PO}_4 \cdot \text{H}_2\text{O}$ ), disodium  
104 hydrogen phosphate dodecahydrate ( $\text{Na}_2\text{HPO}_4 \cdot 12\text{H}_2\text{O}$ ), sodium chloride ( $\text{NaCl}$ ) and sodium  
105 hydroxide ( $\text{NaOH}$ )), active ingredients (caffeine(caf), ibuprofen (ibu), ibuprofen sodium salt  
106 (Na-ibu) ketoprofen (ket) and hydrocortisone (hc), Table 1) and organic solvent employed in  
107 this work (methanol) were purchased from Sigma Aldrich Chemie GmbH (Steinheim,  
108 Germany). Soy phosphatidylcholine (S-100) was a generous gift from Lipoid GmbH  
109 (Ludwigshafen, Germany). 2-hydroxypropyl  $\beta$ -cyclodextrin (HPBCD) with estimated

110 molecular weight of 1396 g/mol and average degree of substitution within 0.5-1.3 (defined as  
 111 unit of 2-hydroxypropyl per glucose unit) was also purchased from Sigma Aldrich or,  
 112 alternatively, from Roquette Freres (Lestrem, France).

113 **Table 1:** Molecular weight (mw), ionization constant (pKa) distribution coefficient at pH 7.4  
 114 (LogD<sub>7.4</sub>), topological polar surface area (TPSA) and molar volume (V<sub>m</sub>) of the investigated  
 115 compounds.

<b>Drug</b>	<b>mw</b> <b>g/mol</b>	<b>pKa</b> <sup>[21]</sup>	<b>LogD</b> <sub>7.4</sub>	<b>TPSA</b> <sup>[21]</sup> <b>Å<sup>2</sup></b>	<b>V<sub>m</sub></b> <sup>[24]</sup> <b>cm<sup>3</sup>/mol</b>
caf	194.2	10.4	-0.03 <sup>[22]</sup>	58.4	133
hc	362.5	-	1.51 <sup>[22]</sup>	98.4	281
Ibu/Na-ibu	206.3/228.3	4.91/≈	1.00 <sup>[23]</sup> /≈	37.3/≈	200/≈
Ket	254.2	4.45	0.19 <sup>[23]</sup>	54.4	212

116

## 117 2.2 UV-visible localized spectroscopy

### 118 2.2.1 API solutions preparation

119 In order to obtain a 73 mM neutral (pH 7.4) and isotonic (280-290 mOsm) phosphate buffer  
 120 saline (PBS), a solution of NaH<sub>2</sub>PO<sub>4</sub>·H<sub>2</sub>O (2.2% W/V) was mixed in a ratio 1:5 with a  
 121 solution of Na<sub>2</sub>HPO<sub>4</sub>·12H<sub>2</sub>O (1.8% W/V). The pH of was subsequently adjusted to 7.3–7.4  
 122 (pH meter Lab 744, Metrohm AG, Herisau, Switzerland) by the addition of NaOH solid  
 123 pellets whereas the tonicity was brought to 280–290 mOsm (Semi-Micro Osmometer K-7400,  
 124 Knauer, Berlin, Germany) by the addition of NaCl solid crystals. Each of the API investigated  
 125 was dissolved in the PBS solution in order to achieve a final drug concentration in the range  
 126 1- 6 mM.

### 127 2.2.2 Cyclodextrin-API samples preparation

128 The complexation studies were conducted following the basic principle of standard phase-  
 129 solubility studies [25] therefore exposing the same amount of API to increasing concentration

130 of the complexing agent. For caffeine, hydrocortisone and ketoprofen, a stock solution of the  
 131 complexing agent (in this work HPBCD) was prepared dissolving approximately 3.6 g of  
 132 cyclodextrin derivative in PBS in order to obtain a 50 mM HPBCD solution. One mL of drug  
 133 solution was mixed together with increasing volumes of HPBCD stock solution (from 0 mL  
 134 up to 1 mL) inside standard Eppendorf vials, in order to achieve a minimum of 5 samples  
 135 with increased cyclodextrin concentration (ranging from 0 mM up to 25 mM) and constant  
 136 API concentration (samples caf<sub>0-4</sub>, hc<sub>0-4</sub>, ibu<sub>0-5</sub>, ket<sub>1-5</sub> in Table 2).

137 **Table 2.** Concentration of active pharmaceutical ingredient (API), 2-hydroxypropyl  $\beta$ -  
 138 cyclodextrin (HPBCD), soy phosphatidylcholine (SPC) and buffer in each of the samples  
 139 investigated. Each sample was analyzed at maximum wavelength of absorption ( $\lambda_{\text{max}}$ ) and the  
 140 local concentration was calculated using its specific API absorptivity ( $\epsilon$ ).

Sample	API conc. mM	HPBCD conc. mM	SPC conc. mM	Buffer conc. mM	$\lambda_{\text{MAX}}$ nm	$\epsilon$ cm <sup>2</sup> / $\mu$ mol
Caffeine						
caf <sub>0</sub>	0.9	-	-	72.8	272	9.7
caf <sub>1</sub>	//	1	-	//	//	//
caf <sub>2</sub>	//	5	-	//	//	//
caf <sub>3</sub>	//	10	-	//	//	//
caf <sub>4</sub>	//	25	-	//	//	//
caf <sub>5</sub>	//	-	25	//	//	//
Hydrocortisone						
hc <sub>0</sub>	0.5	-	-	72.8	247	11.9
hc <sub>1</sub>	//	1	-	//	//	//
hc <sub>2</sub>	//	2.5	-	//	//	//
hc <sub>3</sub>	//	10	-	//	//	//
hc <sub>4</sub>	//	25	-	//	//	//
hc <sub>5</sub>	//	-	25	//	//	//
Ibuprofen						
ibu <sub>0</sub>	1.3	-	-	72.8	221	9.0
ibu <sub>1</sub>	//	0.5	-	//	//	//
ibu <sub>2</sub>	//	1	-	//	//	//
ibu <sub>3</sub>	//	2.5	-	//	//	//
ibu <sub>4</sub>	//	5	-	//	//	//
ibu <sub>5</sub>	//	10	-	//	//	//
ibu <sub>6</sub>	//	-	25	//	//	//
Ketoprofen						
ket <sub>0</sub>	1.4	-	-	72.8	260	16.5

ket <sub>1</sub>	//	0.5	-	//	//	//
ket <sub>2</sub>	//	2.5	-	//	//	//
ket <sub>3</sub>	//	5	-	//	//	//
ket <sub>4</sub>	//	10	-	//	//	//
ket <sub>5</sub>	//	25	-	//	//	//
ket <sub>6</sub>	//	-	25	//	//	//

141

142 For ibu, 0.4 mL of API stock solution in PBS (6.32 mM) were mixed inside standard 2 mL  
 143 Eppendorf vials with increasing volumes (form 0.0 mL to 1.0 mL) of a 20 mM HPBCD PBS  
 144 solution (Table 2). PBS was used in order to fill in the missing volume up to two mL.

145 Samples were stored at room temperature prior to analysis.

### 146 **2.2.3 Liposomes-API samples preparation**

147 A liposomal dispersion was prepared following the standard thin-film hydration method [26].

148 In brief, approximately 2 g soy phosphatidylcholine (S-100) were dissolved into 50 mL of  
 149 methanol in a round bottom flask. The organic solvent was removed by controlled vacuum  
 150 evaporation (25°C; 1 hour; 60–65 mBar final vacuum) employing a Büchi rotary evaporator  
 151 system (model R-124), equipped with a water bath (model B-480) and vacuum pump (model  
 152 V-500; Büchi Labortechnik AG, Flawil, Switzerland). Large liposomes dispersion was  
 153 obtained by reconstituting the lipid film obtained after solvent removal with 50 mL PBS. The  
 154 liposomal dispersion was subsequently extruded throw 800 nm (4 cycles) and 400 nm (4  
 155 cycles) polycarbonate filters (Whatman International Ltd., Bucking-hamshire, UK) in order to  
 156 obtain a homogeneous dispersion of medium-sized liposomes (average diameter  
 157 approximately 400 nm). Prior to analysis, one mL of the liposomal dispersion was mixed with  
 158 1 mL of API solution inside an Eppendorf vial (samples caf<sub>5</sub>, hc<sub>5</sub>, ibu<sub>6</sub> and ket<sub>6</sub> in Table 2).

159 Samples were incubated for 10 min prior to analysis.

### 160 **2.2.4 Analytical method**

161 The analytical method recently introduced by us [20] was employed in this work to  
 162 investigate the influence of cyclodextrins and liposomes on API diffusion in aqueous media.



163 For the spectrophotometric measurements, a double array VWR (VWR International, Radnor,  
164 USA) UV-visible spectrophotometer (model UV-6300 PC) equipped with a Hellma<sup>®</sup>  
165 Suprasil<sup>®</sup> (Sigma-Aldrich) quartz absorption cuvettes (chamber volume of 700  $\mu\text{L}$  and path  
166 length of 10 mm) was employed. Both reference and sample cuvette were filled with the same  
167 volume of distilled water (675  $\mu\text{l}$  and placed in the respective compartment of the  
168 spectrophotometer). At time (t) = 0 sec (starting of the experiment), 25  $\mu\text{L}$  of one sample were  
169 gently injected in the bottom of the sample cuvette by a needle syringe. In order to avoid  
170 evaporation of water, the sample cuvette was sealed with parafilm right after sample injection.  
171 Absorbance readings were recorded at fixed wavelength (corresponding to the  $\lambda_{\text{MAX}}$  of each  
172 of the compounds, Table 2) at regular time intervals (120 sec) for 18 hours at room  
173 temperature (23-24°C). Absorbance was recorded at 0.51 cm from the bottom of the cuvette  
174 ( $h_m$ ).

### 175 **2.2.5 Mathematical data treatment**

176 The mathematical approach previously described by us [20] was employed in order to  
177 calculate both reference diffusivity ( $D_0$ , the diffusivity of the API in absence of solubilizing  
178 vehicles) and apparent diffusivities ( $\bar{D}$ , the diffusivity measured in the presence of  
179 solubilizing vectors). In brief, the spontaneous process of molecules migrating through a  
180 homogeneous medium (in this case water) is described by Equation 2 as:

$$\frac{\partial c(x, t)}{\partial t} = D \frac{\partial^2 c(x, t)}{\partial x^2} \quad \text{Equation 2}$$

181 In this equation, c represents the concentration of the substance (in this case the API  
182 concentration), t the time, x the position, and D the diffusivity.

183 Assuming times (t) and positions (x) such that  $t \ll h^2/D$  and  $x \ll h$  (where h is 3.30 cm, the  
184 full length of the cuvette occupied by water), eq. 2 can be solved analytically as:

$$c(x, t) = \frac{A}{\sqrt{\pi}} \frac{e^{\frac{-x^2}{2\sigma^2 + 4Dt}}}{\sqrt{2\sigma^2 + 4Dt}} \quad \text{Equation 3}$$

185 Where  $\sigma$  represents the width of the initial distribution (considered to be a half gaussian  
 186 curve) and A represents the initial amount of the API. Equation 3 was fitted to the  
 187 experimental data in order to find the best solutions for both D, A and  $\sigma$ .

188 The calculation of constant of equilibrium (K) was based on the assumption that for the 1:1  
 189 complex (L·S) formation between API molecules (i.e. the substrate, S) and a ligand (Eq. 4):



190 For an ideal diluted solution, it can be assumed that the equilibrium constant (K) of  
 191 complexation is given by:

$$K = \frac{[S \cdot L]}{[S][L]} \quad \text{Equation 5}$$

192 Knowing the initial concentration of the ligand ( $L_0$ ), the substrate ( $S_0$ ) and the equilibrium  
 193 concentration of the complex (Q), equation 5 can be re arranged as:

$$K = \frac{Q}{(S_0 - Q)(L_0 - Q)} \quad \text{Equation 6}$$

194 Solving this expression yields two values for Q, whereof only one lies in the range  
 195  $0 \leq Q \leq \min(L_0, S_0)$  (Eq. 7):

$$Q = \frac{1}{2K} \left( 1 + (L_0 + S_0)K - \sqrt{1 + 2(L_0 + S_0)K + (L_0 - S_0)^2 K^2} \right) \quad \text{Equation 7}$$

196 Assuming fast exchange between API in the free and the bound states, the measured value for  
 197 diffusion ( $\bar{D}$ ) will be the weighted average of the diffusions of the free and bound molecules  
 198 ( $D_b$  and  $D_f$  respectively). The relationship between the different diffusivities is described by  
 199 Eq. 8:

$$\bar{D} = MF_b D_b + MF_f D_f = \frac{Q}{L_0} D_b + \left( 1 - \frac{Q}{L_0} \right) D_f = D_f + \frac{Q}{L_0} (D_b - D_f) \quad \text{Equation 8}$$

200 Where  $MF_b$  and  $MF_f$  represent the molar fractions of the bound and free substrate  
201 respectively. Inserting Eq. 7 in Eq. 8 gives a final expression of  $\bar{D}$  as a function of  $L_0$  that can  
202 be fitted to the experimental data (keeping  $S_0$  constant, see section 2..2.2 and Table 2) and  
203 allows for the quantification the diffusivities of bound and free API ( $D_b$  and  $D_f$  respectively).  
204 Partitioning of API into liposomes ( $P_{lip/w}$ ) was calculated using the following equation:

$$P_{lip/w} = \frac{(A_{lip} - A_0)}{A_0} * \frac{V_0}{V_{lip}} \quad \text{Equation 9}$$

205 Where  $A_0$  represents the initial API amount in the reference experiments (i.e. no liposomes),  
206  $A_{lip}$  the amount in the liposomes experiments and  $V_0$  and  $V_{lip}$  represent the liposome-free  
207 volume fraction of the injected volume (estimated to be 22  $\mu\text{L}$ ) and the volume occupied by  
208 the liposomes (estimated to be 3  $\mu\text{L}$ ) respectively.

### 209 **2.3 Nuclear magnetic resonance (NMR) spectroscopy**

210 10  $\mu\text{L}$  of a 7.5 mM Na-ibu non-isotonic PBS solution (10% deuterated water) were added to  
211 590  $\mu\text{L}$  of a 5.7 mM HPBCD non isotonic PBS solution (10% deuterated water) in a standard  
212 5 mm NMR tube, yielding a final solution of concentrations of 0.1 mM and 5.6 mM for Na-  
213 ibu and HPBCD respectively. The NMR experiments were performed employing an Agilent  
214 DD2 NMR (Agilent Technologies, Santa Clara, USA) spectrometer functioning at a proton  
215 frequency of 599.671 MHz. Temperature was stabilized at 30  $^{\circ}\text{C}$  during all experiments.  
216 Diffusion constants were measured using a standard DgsteSL sequence with convection  
217 compensation and treated with the DOSY package.

## 218 **3. Results and discussion**

### 219 **3.1 quantification of diffusion coefficients in absence of binding agents**

220 In table 3 the results from the diffusion studies of the API (caf, hc, ibu and ket) in PBS  
221 solutions without binding agents (i.e. neither HPBCD nor liposomes) are reported. In all  
222 experiments, the data recording position ( $h_m$ ) was used as fixed parameter (0.51 cm) whereas  
223  $A_0$  and  $D_0$  were fitting parameters. The nominal equilibrium concentration ( $c_{eq}$ ) correlates

224 very well ( $R^2$  of 0.99) with  $A_0$ , indication of very good correspondence between experimental  
225 and computational data.

226 **Table 3.** Nominal equilibrium concentration ( $c_{eq}$ ), initial amount ( $A_0$ ), width of the initial  
227 distribution ( $\sigma$ ) and reference diffusivities ( $D_0$ ) of the reference drug (caf, hc, ibu and ket)  
228 samples. All parameters were obtained by fitting the analytical solution of diffusion equation  
229 (Eq. 3) to experimental data of API solutions recorded at  $x=0.51$ cm.

Sample	$c_{eq}$ (mM)	$A_0$	$\sigma$	$D_0$ ( $10^{-6}$ cm <sup>2</sup> /sec)
caf <sub>0</sub>	0.03	0.231	0.104	9.120
hc <sub>0</sub>	0.02	0.145	0.111	6.442
ibu <sub>0</sub>	0.05	0.331	0.101	7.788
ket <sub>0</sub>	0.05	0.408	0.055	7.724

230 The Stokes-Einstein equation relates the diffusion constant ( $D$ ) to the radius of a hypothetical  
231 sphere ( $r$ ), the temperature ( $T$ ) and the viscosity ( $\eta$ ) via (Eq. 10):

$$D = \frac{k_B T}{6\pi\eta r} \quad \text{Equation 10}$$

232 Where  $k_B$  is Boltzmann's constant. Assuming that all the experiments are performed at the  
233 same temperature ( $T$ ) and that concentration of the API is so low that the viscosity ( $\eta$ ) is not  
234 affected we can expect a linear correlation between molar volume ( $V_m$ , Table 1) and  $D_0$ .  
235 Diffusion coefficient values are consistent with previous finding [20] and indeed, fitting  $D_0$  to  
236 the estimated molar volumes yields a straight line ( $R^2=0.99$ ). Hydrocortisone is the largest  
237 molecule within the investigated series ( $V_m$  of 281 cm<sup>3</sup>/mol, Table 1) and because of that it  
238 shows the lowest  $D_0$  ( $6.4 * 10^{-6}$  cm<sup>2</sup>/sec) whereas caffeine, that is the smallest of the  
239 investigated compounds ( $V_m$  of 133 cm<sup>3</sup>/mol), expresses the highest  $D_0$  ( $9.2 * 10^{-6}$  cm<sup>2</sup>/sec).  
240 Ibuprofen and ketoprofen have very similar  $V_m$  (200 and 212 cm<sup>3</sup>/mol) in between caffeine  
241 and hydrocortisone and this is reflected in similar diffusivities ( $7.8$  and  $7.7 * 10^{-6}$  cm<sup>2</sup>/sec

242 respectively) comprised between the other two compounds (Table 3). The data reported in  
 243 Table 3 are fundamental as they are the reference data to which experimental data collected  
 244 from samples with solubilizing vehicles should be compared with.

### 245 3.2 Diffusion coefficients in the presence of HPBCD

246 **Table 4.** Nominal equilibrium concentration ( $c_{eq}$ ), calculated initial amount (A), width of the  
 247 initial distribution ( $\sigma$ ) and relative diffusivities ( $\bar{D}$ ) of the investigated compounds (caf, hc, ibu  
 248 and ket) in the presence of increasing concentration of HPBCD.

Sample	HPBCD conc. (mM)	$C_{eq}$ (mM)	A	$\sigma$	$\bar{D}$ ( $10^{-6} \text{ cm}^2/\text{sec}$ )
Caffeine					
caf <sub>1</sub>	1	0.03	0.233	0.105	9.089
caf <sub>2</sub>	5	//	0.223	0.104	8.335
caf <sub>3</sub>	10	//	0.220	0.103	8.070
caf <sub>4</sub>	25	//	0.221	0.104	7.924
Hydrocortisone					
hc <sub>1</sub>	1	0.02	0.132	0.119	5.149
hc <sub>2</sub>	2.5	//	0.134	0.110	4.092
hc <sub>3</sub>	10	//	0.135	0.122	3.415
hc <sub>4</sub>	25	//	0.132	0.121	3.400
Ibuprofen					
ibu <sub>1</sub>	0.5	0.05	0.319	0.115	5.760
ibu <sub>2</sub>	1	//	0.327	0.125	5.265
ibu <sub>3</sub>	2.5	//	0.312	0.134	3.787
ibu <sub>4</sub>	5	//	0.323	0.125	3.554
ibu <sub>5</sub>	10	//	0.334	0.122	3.110
Ketoprofen					
ket <sub>1</sub>	0.5	0.05	0.389	0.062	6.828
ket <sub>2</sub>	2.5	//	0.372	0.096	5.468
ket <sub>3</sub>	5	//	0.342	0.114	4.796
ket <sub>4</sub>	10	//	0.357	0.122	4.061

ket <sub>5</sub>	25	//	0.326	0.125	3.213
------------------	----	----	-------	-------	-------

---

Data recorded at x=0.51 cm

249 Fig. 1 reports the experimental data (blue line) and fit (red line) of ibuprofen in the presence  
 250 of increasing HPBCD concentration (Fig. 1, ibu<sub>0</sub>-ibu<sub>5</sub>). The other compounds show similar  
 251 behavior. The diffusion profiles change when the concentration of the binding agent is  
 252 increased. Specifically, the slope of the rising section of the curves decreases whereas the  
 253 curvature at the top becomes more gentle and the time where the maximum occurs ( $t_{max}$ )  
 254 increases. The fitting of Eq. 3 to the experimental data was very good in all circumstances and  
 255 in accordance with our previous work (fitting error below 1%, [20]). In Table 4 the initial  
 256 amount (A) and diffusivities ( $\bar{D}$ ) obtained from the data fitting are reported for each of the  
 257 API investigated.

258 It should be highlighted that, for all drugs, increasing the HPBCD concentration results in a  
 259 decrement in diffusivities, showing that all compound bind to HPBCD. The magnitude of the  
 260 variation depends on the binding constant and varies significantly between the investigated  
 261 compounds. For instance, in the case of caffeine, even at the highest concentration of HPBCD  
 262 (25 mM) the relative diffusion identified is only 14 % lower than  $D_0$  (Table 3 and 4). For all  
 263 the other compounds, the impact of cyclodextrins on API diffusion is much more severe. At  
 264 the highest concentration of HPBCD (25 mM), the decrease in diffusivities exceeds 50 % in  
 265 the case of ibuprofen and hydrocortisone whereas for ketoprofen it is 47%. This data gives a  
 266 picture of what is happening when cyclodextrins bind an API. As the HPBCD-API complex is  
 267 larger than the API alone, we expect the complex to diffuse slower than the free API, as  
 268 indeed is the case. In other words, binding with cyclodextrins has a negative effect on the net  
 269 drug transport through the UWL. This results are in agreement with previous findings [15-17].  
 270 The data obtained in this work give also a better and clearer picture of the reason why drug  
 271 transport of drugs through UWL is affected by the presence of solubilizing vehicles such as

272 cyclodextrins. From the data obtained in this work it is evident that for hydrocortisone, but  
273 also for the ionizable compound ibu, the gradient of concentration is produced by both free  
274 and complexed API molecules. This is demonstrated by the fact that the estimated initial drug  
275 amount of API (A) does not change significantly with increased concentration of HPBCD  
276 (Table 4, and therefore with increased API-HPBCD complexation) in the UWL. Moreover,  
277 these findings are in partial agreement with Stewart at al. [19] where they found that the net  
278 flux of itraconazole through a biomimetic barrier was proportional to the total apparent  
279 solubility of the drug in the donor (i.e. both bound and unbound API fraction in solution).  
280 However, in the present work, the total flux of all APIs investigated resulted reduced through  
281 the UWL and not improved by the presence of a solubilizer. This is already an interesting  
282 findings that exclude the role of concentration gradient as the responsible for the reduction of  
283 API flux observed. In the case of ketoprofen, there is a clear trend in reduction in A with  
284 increased HPBCD concentration (Table 4) and this could indicate that there is a decrease in  
285 ket molecules available with increased HPBCD. This could be explained by the formation of  
286 macromolecular aggregates [27] that reduces the initial concentration gradient (driving force  
287 of passive diffusion). From these data it is clear that, especially with compounds forming  
288 stable complex with HPBCD, the complex API-HPBCD is maintained also in diluted  
289 conditions (i.e. after injection), and this fact produces the reduction of API diffusing through  
290 the UWL measured. It is evident from these data that, and agreement with previous findings  
291 [15-17], cyclodextrins clearly hamper the diffusion of API through the UWL. In partial  
292 disagreement with previous reports [15] however, it appears that also hydrophilic compounds  
293 (in this case caffeine), are affected in their diffusion through the UWL at high concentration  
294 of HPBCD, even though the binding constant of caffeine to HPBCD is low [28].

### 295 **3.3 calculation of $K$ , $D_f$ and $D_b$**

296 The decrease of the relative diffusion coefficient measured when the API are complexed with  
 297 cyclodextrin depends on the binding constant. After injection at the bottom of the cuvette, free  
 298 API molecules, free HPBCD and API-HPBCD complex will start to diffuse. In accordance  
 299 with Stokes-Einstein equation (Eq. 10), assuming similar experimental conditions (absolute  
 300 temperature (T) and viscosity of the media ( $\eta$ )) in each experiment, the free API and API-  
 301 HPBCD complexes will show different diffusivities ( $D_f$  and  $D_b$  respectively) determined by  
 302 their size (hydrodynamic radius (r)).

303 In Fig. 2 the relationship between apparent diffusivity ( $\bar{D}$ ) and HPBCD concentration is  
 304 reported for all the compound investigated. Fitting the experimental data with equation 8 and  
 305 9 (red line, Fig. 2) it is possible to obtain numerical values for the equilibrium constant (K)  
 306 and the diffusivities of bound and free API ( $D_b$  and  $D_f$  respectively). The results are reported  
 307 in Table 5.

308 **Table 5.** Equilibrium constant (K), diffusivity of free API ( $D_f$ ) and complexed API ( $D_b$ )  
 309 identified for each of the investigated compound (caf, hc, ibu, ket) in the experiment  
 310 performed in the presence of HPBCD.

API	K M <sup>-1</sup>	D <sub>f</sub> 10 <sup>-6</sup> cm <sup>2</sup> /sec	D <sub>b</sub> 10 <sup>-6</sup> cm <sup>2</sup> /sec
caf	243 ± 151	9.2 ± 0.1	7.6 ± 0.3
hc	1028 ± 246	6.5 ± 0.1	3.2 ± 0.1
ibu	4058 ± 2890	7.6 ± 0.3	3.1 ± 0.3
ket	381 ± 102	7.5 ± 0.2	2.9 ± 0.3

311  
 312 For all compounds,  $D_f$  is very similar to  $D_0$  (Table 3, discrepancy of 1%). Moreover, the  
 313 equilibrium constants obtained are in good agreement with literature data [15, 28-31]. Ibu and  
 314 hc are the compounds with the strongest equilibrium constant and therefore their diffusion  
 315 through the UWL is most affected. For ibu, ket and hc,  $D_b$  is close to  $3 \cdot 10^{-6}$  cm<sup>2</sup>/sec. This  
 316 value seems very reasonable, as the size of the inclusion complex API-HPBCD is mostly due



317 to the cyclodextrin (Mw of 1.4 kDa) and DOSY NMR results showed that the diffusion  
318 constant for HPBCD in water is  $2.9 \cdot 10^{-6} \text{ cm}^2/\text{s}$ . Moreover, NMR results with Na-ibu  
319 evidenced that API-HPBCD complex diffuses at the same rate as HPBCD alone. Caffeine  
320 expresses a much higher value for  $D_b$  (over  $7 \cdot 10^{-6} \text{ cm}^2/\text{sec}$ ). Theoretically, this value should  
321 be much lower and close to  $3 \cdot 10^{-6} \text{ cm}^2/\text{sec}$  (as with the other API investigated). It is quite  
322 plausible that the Caf-HPBCD complex is more affected than the others by rapid on-and-off  
323 kinetics (due to poor complex stability, see equilibrium constant values in table 5). This fact  
324 makes a correct estimation of  $D_b$  impossible with the current technique, and this might be an  
325 issue for all complexes with low K. We are aware that the obtained value lies outside the  
326 expected range and will investigate the system further in the near future. From these data we  
327 can anyway conclude that measured reduction in API flux through the UWL in the presence  
328 of HPBCD is not due to a reduction in the concentration gradient but it is mostly due to the  
329 reduction in relative diffusivity of API. In fact, API-HPBCD complexes diffuse much slower  
330 through the UWL than free APIs ( $D_b \ll D_f$ , see Table 5), therefore  $\bar{D}$  will decrease with  
331 increasing concentration of HPBCD. This reduction in apparent diffusivity is, in practice,  
332 directly corresponding to a reduction in the amount of API passing through the UWL. It  
333 appears also clear from our results that the more stable the complex API-HPBCD is (i.e.  
334 higher is K), the more significant this phenomenon will be.

### 335 **3.4 Partitioning and relative diffusivities**

336 The experiments involving liposomes were conducted similarly to the cyclodextrins ones but  
337 in this case each of the API was incubated for 10 minutes previous injection in the cuvette  
338 with a liposomal dispersion containing 25 mM phosphatidylcholine S-100 of 400 nm average  
339 diameter. In this case, liposomes due to their sizes ( $d_m = 400 \text{ nm}$ ) were located on the bottom  
340 of the cuvette for the duration of the experiment, differently from the cyclodextrin  
341 experiments where the API-HPBCD complexes were also diffusing. For all compounds

342 investigated, a reduction in apparent mass transport of API through the UWL was measurable  
343 when liposomes were present. The fitting to the experimental data in this case reveals that,  
344 differently from cyclodextrins, the initial amount of API measured ( $A$ ) was reduced after 10  
345 min incubation with liposomes for ketoprofen, ibuprofen and hydrocortisone but not for  
346 caffeine. Since the experimental set up used was a closed system (i.e. mass preservation) it  
347 can be assumed that all the material that did not diffuse through the cuvette was sequestered  
348 by the phospholipid bilayers. Interestingly, liposomes did not only incorporate significant  
349 amount of API molecules, but they also affect the apparent diffusivity ( $\overline{D}$ ) of each of the  
350 compounds investigated (i.e. liposomes strongly retain API). This indicated that, as drug  
351 diffusion occurs, the drug is release again, but with a kinetics proportional to the affinity of  
352 the API for the phospholipid bilayers (indicatively expressed by the  $\text{Log}D_{7.4}$ , Table 1). In Fig.  
353 3, the liposome/water partition coefficient ( $P_{\text{lip/w}}$ , gray column) calculated accordingly to Eq.  
354 9 as well as the apparent diffusivities measured (blue dots) are reported for each of the drugs.  
355 As it can be seen, hc is the most incorporated compound into the phospholipid bilayer (Fig.  
356 3), with an almost 4 times higher distribution of API molecules in the lipophilic bilayer in  
357 comparison to the water phase. Ibu and ket show very comparable behaviors, as expected  
358 from the molecular physicochemical properties (comparable  $\text{pK}_a$  (Table 1) and chemical  
359 structure). For both drugs, molecules distribute approximately two times more in the lipid  
360 phase than in the water phase. Caffeine is quite hydrophilic (negative  $\text{log}D_{7.4}$ , Table 1) and  
361 therefore its very low partition into lipophilic environment is not surprising. The experimental  
362 approach utilized in this work gives additive information on the relative diffusivities of the  
363 API in the presence of liposomes. From the results reported in Fig. 3, it is evident that also  
364 relative diffusivities of API are reduced by the presence of liposomes, also for hydrophilic  
365 compound. For example, caf relative diffusivity is reduced by approx. 20% in comparison to  
366  $D_0$  (Table 2) whereas hc diffusivity is reduced down to 55% of its reference diffusion (Table

367 2). These data allow to make some interesting considerations. First, interaction of API  
368 molecules with phospholipid bilayers are extremely fast as equilibrium is reached within 10  
369 min. Second, in the case of phospholipid vesicles, it is clear that the reduction in apparent flux  
370 of API through UWL is affected by the reduction in concentration gradient induced ( $dc/dx$ ) by  
371 the segregation of drug molecules into liposomes. Unfortunately, in the case of liposomes it  
372 was not possible to estimate a real equilibrium constant API-liposome as in the case of  
373 HPBCD, since the stoichiometry of reaction API-liposomes was unknown. However, using as  
374 parameter the variation within relative diffusivity ( $\bar{D}$ ) and reference diffusivity ( $D_0$ ) it is  
375 possible to estimate that the binding between hc and the phospholipid bilayers should be  
376 approx. two-times stronger than ibuprofen and ketoprofen and almost three-times stronger  
377 than with caffeine.

#### 378 **4. Conclusion**

379 In this work the interaction of four APIs with classical solubilizing vehicles (cyclodextrins  
380 and liposomes) has been successfully studied in unstirred aqueous conditions. The transport  
381 through the UWL of drug molecules is significantly affected by the presence of both  
382 cyclodextrins and liposomes. The extent is connected to the intrinsic physicochemical  
383 properties of API molecules. Specifically, the diffusivity of small hydrophilic compounds  
384 such as caffeine is not strongly hampered by the presence of solubilizing vehicles whereas, for  
385 compounds with higher lipophilicity (ibuprofen, ketoprofen and hydrocortisone), the  
386 reduction in transport rate results quite remarkable. In both cases (HPBCD and liposomes) the  
387 diffusion of drug through UWL is limited by drug sequestration and consequent reduced mass  
388 flux. In the case of cyclodextrins, empirical data are the results of the diffusion of both free  
389 drug and drug-HPBCD complex whereas, in the case of liposomes, the experimental data  
390 reassemble the diffusion of the free drug only, as we can assume that the liposomes are  
391 stationary (on the relevant time scales). This is due to the much slower diffusivity of

392 liposomes in respect to drug molecules. In both cases however, the mathematical approach  
393 used results efficient in order to obtain reliable information on passive drug diffusion through  
394 UWL in presence of solubilizing agents.

395 **References**

- 396 [1] S. Kalepu, V. Nekkanti, Insoluble drug delivery strategies: review of recent advances and  
397 business prospects, *Acta Pharm. Sin. B* 5 (2015) 442-453.
- 398 [2] R. Liu, *Water insoluble drug formulations*, second ed., CRS Press, Boca Raton, 2008.
- 399 [3] M.E. Brewster, T. Loftsson, Cyclodextrins as pharmaceutical solubilizers, *Adv. Drug*  
400 *Deliv. Rev.* 2007 (59) 645–666.
- 401 [4] G. Bozzuto, A. Molinari, Liposomes as nanomedical devices, *Int. J. Nanomedicine* 10  
402 (2015) 975-999.
- 403 [5] M.P. di Cagno, The potential of cyclodextrins as novel active pharmaceutical ingredients:  
404 a short overview, 22 (2017) doi:10.3390/molecules22010001.
- 405 [6] M.P. di Cagno, J. Styskala, J. Hlaváč, M. Brandl, A. Bauer-Brandl, N. Skalko-Basnet,  
406 Liposomal solubilization of new 3-hydroxy-quinolinone derivatives with promising  
407 anticancer activity: a screening method to identify maximum incorporation capacity, *J.*  
408 *Liposome Res.* 21 (2011) 272-278.
- 409 [7] K.A. Connors, The stability of cyclodextrin complexes in solution, *Chem. Rev.* 97 (1997)  
410 1325-1357.
- 411 [8] R. Carrier, L.A. Miller, I. Ahmed, The Utility of cyclodextrins for enhancing oral  
412 bioavailability, *J. Control. Release* 123 (2007) 78-99
- 413 [9] K. Sugano, K. Terada, Rate and extent-limiting factors of oral drug absorption: theory and  
414 applications, *J. Pharm. Sci.* 104 (2015) 2777-2788.
- 415 [10] G.L. Flynn, S.H. Yalkowsky, Correlation and prediction of mass transport across  
416 membranes I: influence of alkyl chain length on flux determining properties of barrier and  
417 diffusant, *J. Pharm. Sci.* 61 (1972) 838-852.
- 418 [11] T. Korjamo, A. Heikkinen, J. Mönkkönen, Analysis of unstirred water layer in in vitro  
419 permeability experiments, *J. Pharm. Sci.* 98 (2009) 4469-4479.

420 [12] Sugano et al. Biopharmaceutics Modeling and Simulations: Theory, Practice, Methods,  
421 and Applications, John Wiley & Sons, Hoboken 2012

422 [13] A. Avdeef, Absorption and Drug Development: Solubility, Permeability, and Charge  
423 State, John Wiley & Sons, Hoboken 2003

424 [14] P.H. Barry, J.M. Diamond, Effects of unstirred layers on membrane phenomena,  
425 *Physiol. Rev.* 64 (1984) 763-871.

426 [15] M.C. Brewster, M. Noppr, J. Peeters, T. Loftsson, Effect of the unstirred water layer on  
427 permeability enhancement by hydrophilic cyclodextrins, *Int. J. Pharm. Sci.* 342 (2007) 250-  
428 253.

429 [16] A. Dahan, J.M. Miller, A. Hoffman, G.E. Amidon, G.L. Amidon, The solubility-  
430 permeability interplay in using cyclodextrins as pharmaceutical solubilizers: mechanistic  
431 modeling and application to progesterone, *J. Pharm. Sci.* 99 (2010) 2739-2749.

432 [17] A. Dahan, J. Miller, The solubility-permeability interplay and its implication in  
433 formulation design and development for poorly soluble drugs, *AAPS J.* 14 (2012) 244-250.

434 [18] N. Fine-Shamir, A. Beig, M. Zur, D. Lindley, J.M. Miller, A. Dahan, toward successful  
435 cyclodextrin based solubility-enabling formulations for oral delivery of lipophilic drugs:  
436 solubility–permeability trade-off, biorelevant dissolution, and the unstirred water layer, *Mol-  
437 Pharm.* 14 (2017) 2138–2146

438 [19] A.M. Stewart, M.. E. Grass, D.M., Mudie, M.M. Morgen, D.T. Friesen, D.T. Vodak,  
439 Development of a biorelevant, material-sparing membrane flux test for rapid screening of  
440 bioavailability-enhancing drug product formulations, *Mol. Pharm.* 14 (2017) 2032-2046.

441 [20] M.P. di Cagno, F. Clarelli, J. Våbenø, C. Lesley, S.D. Rahman, J. Cauzzo, E.  
442 Franceschinis, N. Realdon, P.C. Stein, Experimental determination of drug diffusion  
443 coefficients in unstirred aqueous environments by temporally resolved concentration  
444 measurements, *Mol. Pharm.* 15 (2018) 1488-1494.

445 [21] Pubchem. <https://pubchem.ncbi.nlm.nih.gov>, 2018 (accessed 28 July 2018).

446 [22] Y.W. Alelyunas, L. Pelosi-Kilby, P. Turcotte, M. Kary, R.C. Spreen, A high throughput  
447 dried DMSO LogD lipophilicity measurement based on 96-well shake-flask and atmospheric  
448 pressure photoionization mass spectrometry detection, *J. Chromatogr. A* 1217 (2010) 1950-  
449 1955.

450 [23] P.C. Stein, M. di Cagno, A. Bauer-Brandl, A novel method for the investigation of  
451 liquid/liquid distribution coefficients and interface permeabilities applied to the water-  
452 octanol-drug system, *Pharm. Res.* 28 (2011) 2140-2146.

453 [24] United States Environmental Protection Agency, <https://comptox.epa.gov/dashboard>  
454 2018 (accessed 28 July 2018).

455 [25] T. Higuchi, K.A. Connors, Phase-solubility techniques, in: C.N. Reilley (Eds.), *Advances*  
456 *in Analytical Chemistry and Instrumentation*, John Wiley & Sons, Inc., Hoboken, 1965, pp.  
457 117–212.

458 [26] A. Samad, S. Aqil, M. Aqil, Liposomal drug delivery systems: an update review, *Curr.*  
459 *Drug Deliv.* 4 (2007) 297-305.

460 [27] T. Loftsson, A. Magnúsdóttir, M. Másson, F. Sigurjónsdóttir, Self-association and  
461 cyclodextrin solubilization of drugs, *J. Pharm. Sci.* 91 (2002) 2307–2316.

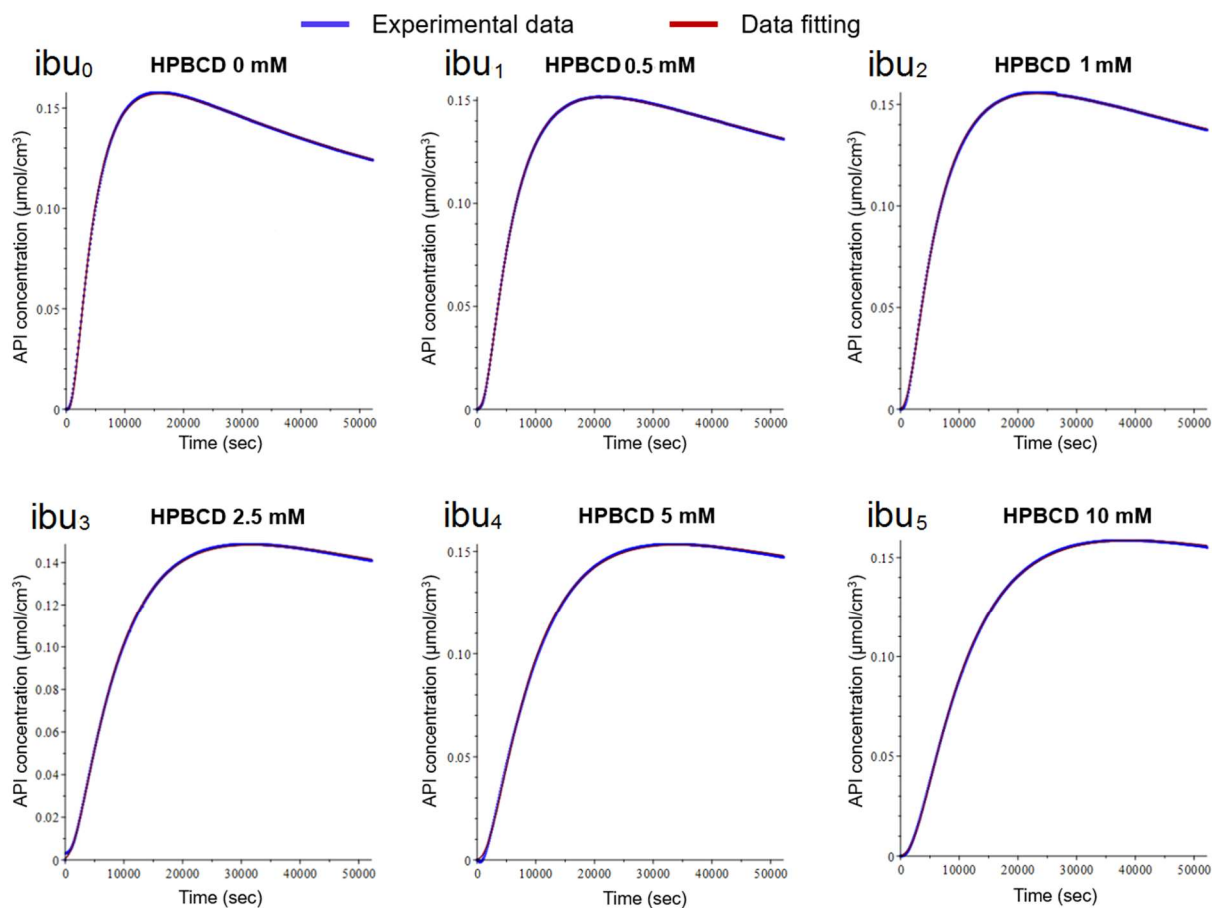
462 [28] E. Aircart, E. Junquera, Complex formation between purine derivatives and  
463 cyclodextrins: a fluorescence spectroscopy study, *J. Incl. Phenom. Macrocycl. Chem.* 47  
464 (2003) 161-165.

465 [29] S. Sridevi, P.V. Diwan, Optimized transdermal delivery of ketoprofen using pH and  
466 hydroxypropyl- $\beta$ -cyclodextrin as co-enhancers, *Eur. J. Pharm. Biopharm.* 54 (2002) 151–154.

467 [30] M.P. Di Cagno, P.C. Stein, N. Skalko-Basnet, M. Brandl, A. Bauer-Brandl,  
468 Solubilization of ibuprofen with  $\beta$ -cyclodextrin derivatives: energetic and structural studies, *J.*  
469 *Pharm. Biomed. Anal.* 55 (2011) 446-451.

470 [31] T. Loftsson, S.T. Vogenes, M.E. Brewster, F. Konrádsdóttir, Effects of cyclodextrins on  
471 drug delivery through biological membranes, *J. Pharm. Sci.* 2007 96 (2007) 2532-2546.  
472

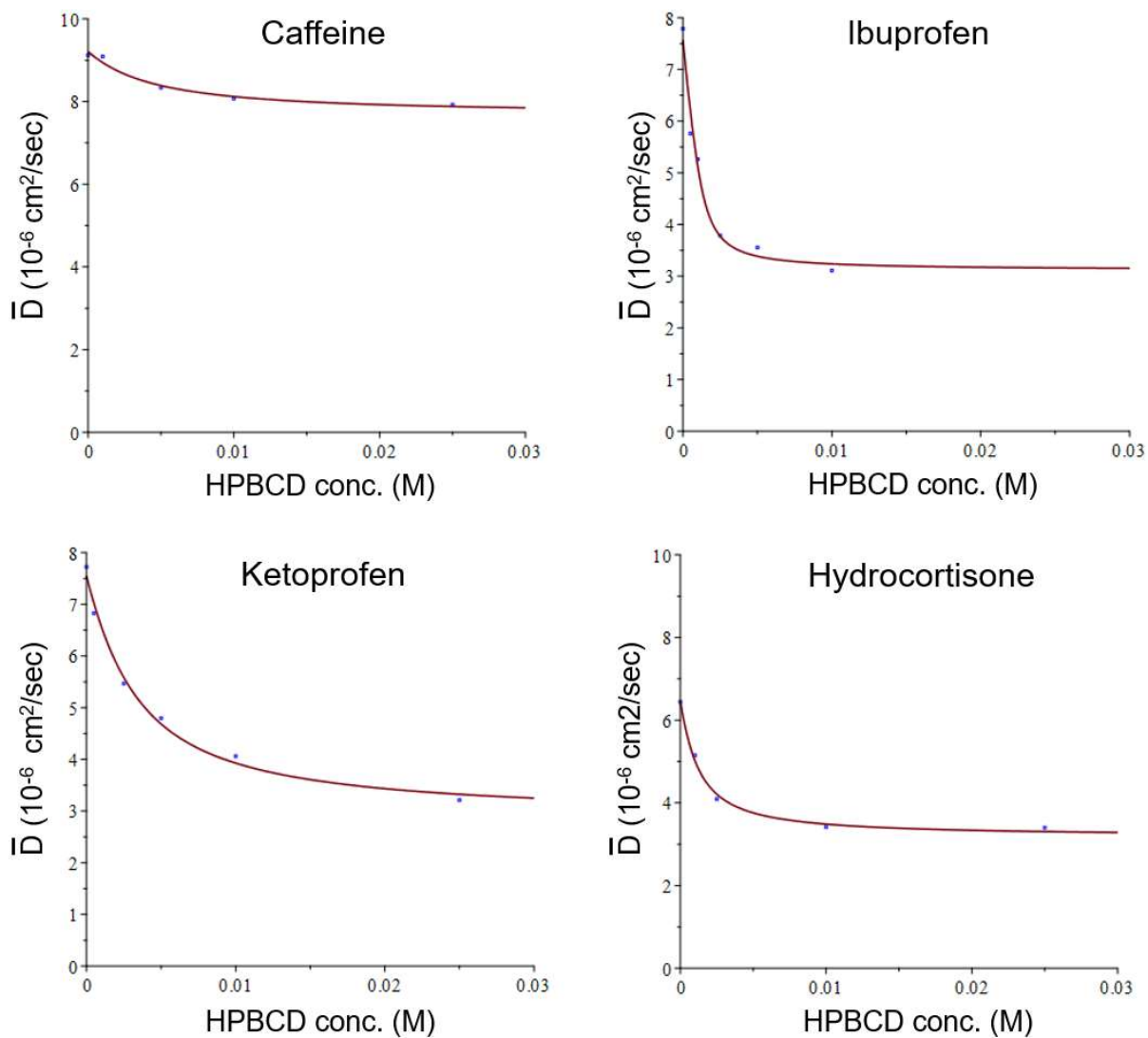




473

474 **Figure 1.** Diffusion profiles of ibuprofen through the unstirred water layer in absence ( $ibu_0$ )  
 475 and in the presence ( $ibu_1$  to  $ibu_5$ ) of increasing concentration (from 1 mM to 10 mM) of  
 476 hydroxypropyl- $\beta$ -cyclodextrin. The blue lines represent the experimental data recorded at 0.51  
 477 cm from origin of diffusion whereas the red lines represent the data fitting.

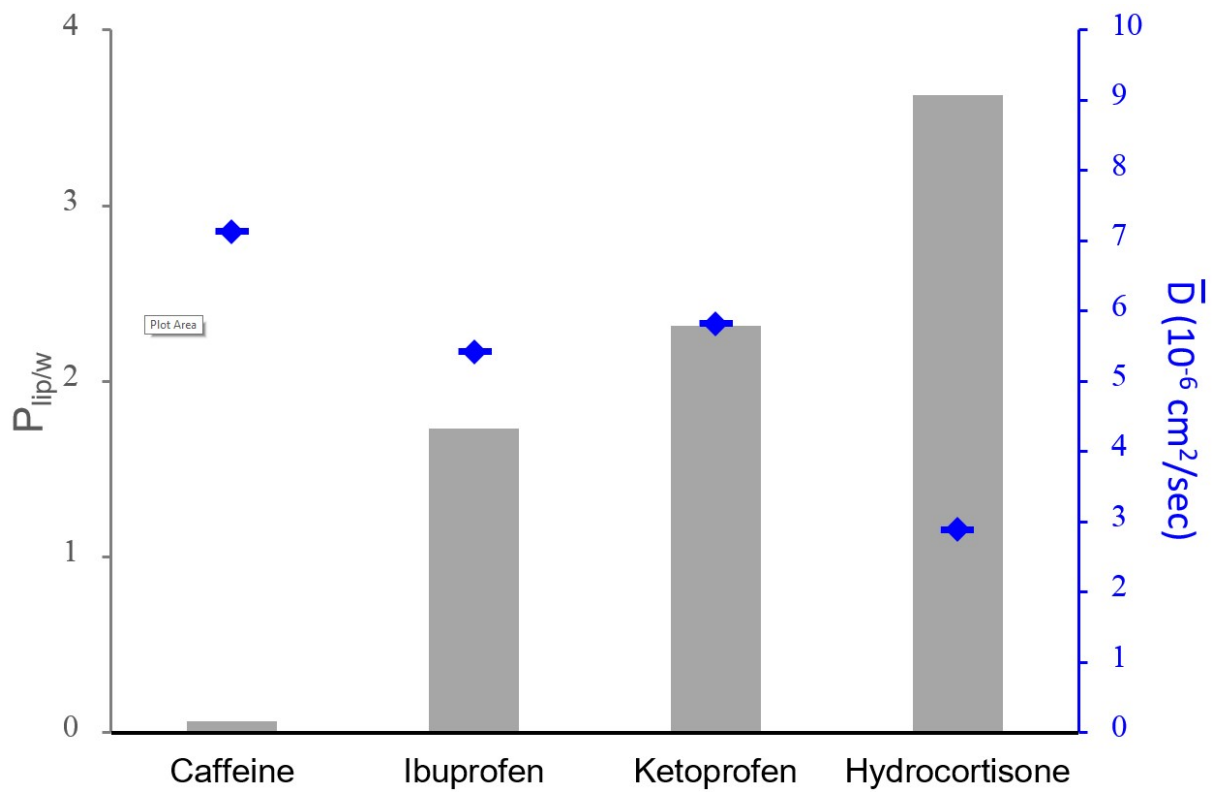
478



479

480 **Figure 2.** Relationship between relative diffusion coefficient ( $\bar{D}$ ) and hydroxypropyl- $\beta$ -  
 481 cyclodextrin (HPBCD) concentration for all the investigated compounds. The red line  
 482 represents the data fitting of Eq. 7-8 to experimental values.

483



484

485 **Figure 3.** Partition coefficient liposomes/water ( $P_{lip/w}$ ) and relative diffusion coefficients ( $\bar{D}$ )  
 486 measured for all investigated compounds in the experiments performed in the presence of  
 487 phospholipid vesicles (25 mM phosphatidylcholine S-100 concentration, liposomes diameter of  
 488 400 nm).

489

490